RadioGraphics

Combined PET-CT in the Head and Neck

Part 1. Physiologic, Altered Physiologic, and Artifactual FDG Uptake[1]

Todd M. Blodgett, MD • Melanie B. Fukui, MD • Carl H. Snyderman, MD • Barton F. Branstetter IV, MD • Barry M. McCook, MD • Dave W. Townsend, PhD • Carolyn C. Meltzer, MD

ONLINE-ONLY CME

See www.rsna.org/education/rg_cme.html.

LEARNING OBJECTIVES

After reading this article and taking the test, the reader will be able to:

- Discuss the common physiologic FDG uptake patterns and variants in the head and neck.
- List several nonmalignant causes of FDG uptake in the neck.
- Describe the most common artifacts encountered in the head and neck region, including attenuation correction artifacts.

Positron emission tomography (PET) with 2-[fluorine-18] fluoro-2-deoxy-D-glucose (FDG) has been effective for the diagnosis, staging, and restaging of malignancies of the head and neck region. However, lack of anatomic landmarks, variable physiologic uptake, and asymmetric FDG distribution in several altered physiologic states can confound image interpretation. In addition, many benign causes and several artifacts can simulate physiologic or pathologic FDG uptake in the head and neck. Combined PET–computed tomography (CT) is a unique imaging modality that permits anatomic and functional imaging on a single scanner with nearly perfect coregistration. Combined PET-CT provides information that cannot be obtained with PET or CT alone. In particular, PET-CT facilitates the interpretation of FDG uptake in the head and neck, an area that is characterized by dense and complex anatomic structures. An atlas of FDG uptake in this anatomic region was compiled on the basis of combined PET-CT findings in 11,000 patients. In general, patterns of FDG uptake were variable and often reflected patient activity during or immediately preceding the uptake phase. With the growing interest in PET-CT, interpreting radiologists and nuclear medicine physicians must be familiar with the patterns of FDG uptake in the head and neck to avoid misinterpretation or misdiagnosis.

Abbreviation: FDG = 2-[fluorine-18] fluoro-2-deoxy-D-glucose

RadioGraphics 2005; 25:897–912 • **Published online** 10.1148/rg.254035156 • **Content Codes:** HN NR NM

[1]From the Departments of Radiology (T.M.B., B.F.B., B.M.M., D.W.T., C.C.M.), Otolaryngology (C.H.S., B.F.B.), Psychiatry (C.C.M.), and Neurology (C.C.M.), University of Pittsburgh, 200 Lothrop St, Pittsburgh, PA 15213; and the Department of Radiology, Allegheny General Hospital, Pittsburgh, Pa (M.B.F.). Presented as an education exhibit at the 2001 RSNA Annual Meeting. Received June 26, 2003; revision requested October 22; final revision received October 25, 2004; accepted November 3. T.M.B. is a consultant for Petnet Pharmaceuticals; D.W.T. is a consultant for CPS Innovations; all remaining authors have no financial relationships to disclose. **Address correspondence to** T.M.B. (e-mail: *Blodgetttm@msx.upmc.edu*).

See Fukui et al (pp 913–930) for Part 2 of this two-part series of articles.

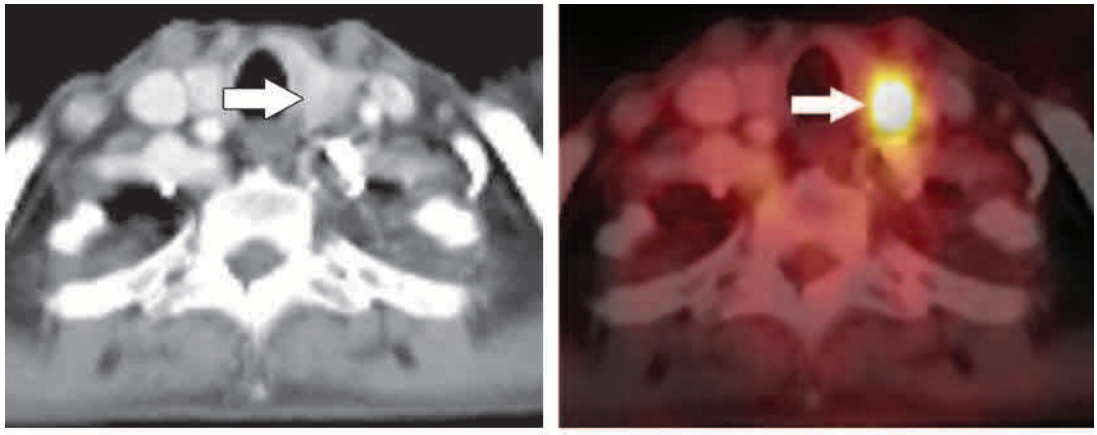

a. b.

Figure 1. Hypermetabolic thyroid adenoma. Axial CT **(a)** and fused PET-CT **(b)** scans show focal intense FDG uptake (arrow) that is localized to the left lobe of the thyroid gland. Subsequent biopsy helped confirm thyroid adenoma.

Introduction

Positron emission tomography (PET) with 2-[fluorine-18] fluoro-2-deoxy-D-glucose (FDG) has been used to successfully diagnose, stage, and restage head and neck cancer (1–5). FDG PET is more sensitive and specific than computed tomography (CT) or magnetic resonance imaging in the detection of recurrent neoplasm. However, if PET alone is performed, limited spatial resolution and lack of anatomic landmarks hinder accurate tumor localization, particularly in the dense and complex anatomic structures of the head and neck. In addition, variable FDG uptake in normal structures such as the nasal turbinates, pterygoid muscles, extraocular muscles, parotid and submandibular glands, and lymphoid tissue in the Waldeyer ring may confuse interpretation and lead to false-positive results (6). Although FDG uptake in primary neoplasms is usually greater than that observed in even the most metabolically active normal structures, overlap between tumor and physiologic uptake may confound interpretation.

Often, the interpreting physician relies on symmetry or location to differentiate between physiologic and pathologic FDG accumulation. However, symmetry is not a reliable indicator of physiologic processes. Several malignancies can manifest with strikingly symmetric FDG uptake; conversely, physiologic uptake will often be asymmetric.

Furthermore, symmetry is not a reliable indicator in postsurgical patients. For example, vocal cord paralysis from prior neck surgery can cause superphysiologic FDG uptake on the contralateral side, from compensatory effort in the unaffected cord. Another interpretive pitfall is seen in patients who have undergone removal of a gland or muscle. The normal physiologic FDG uptake in the remaining gland or muscle can have an asymmetric appearance.

Patients are generally instructed to remain quiet during the FDG uptake phase to limit physiologic vocal cord uptake. Other interventions, such as sedation or neck collars, help minimize physiologic uptake in the head and neck (7,8). In general, however, these protocols are inconvenient for the patient, and they do not eliminate physiologic uptake entirely.

Several limitations of PET in patients with malignancies of the head and neck have been overcome with in-line sequential combined PET-CT. This novel modality allows reliable coregistration of anatomic and functional data. CT attenuation, rather than transmission scan data, is used for attenuation correction of emission data (9). Although combined PET-CT has undoubtedly facilitated the differentiation of physiologic from pathologic processes, there are new artifacts unique to this modality (10,11).

To effectively and accurately interpret PET or fused PET-CT scans, a comprehensive knowledge of physiologic and altered physiologic FDG uptake in the head and neck, as well as an awareness of potential modality-specific artifacts, is essential. In this article, we discuss and illustrate a broad spectrum of these uptake patterns, including uptake in glands (thyroid gland, salivary glands), muscles (muscles of the neck and face,

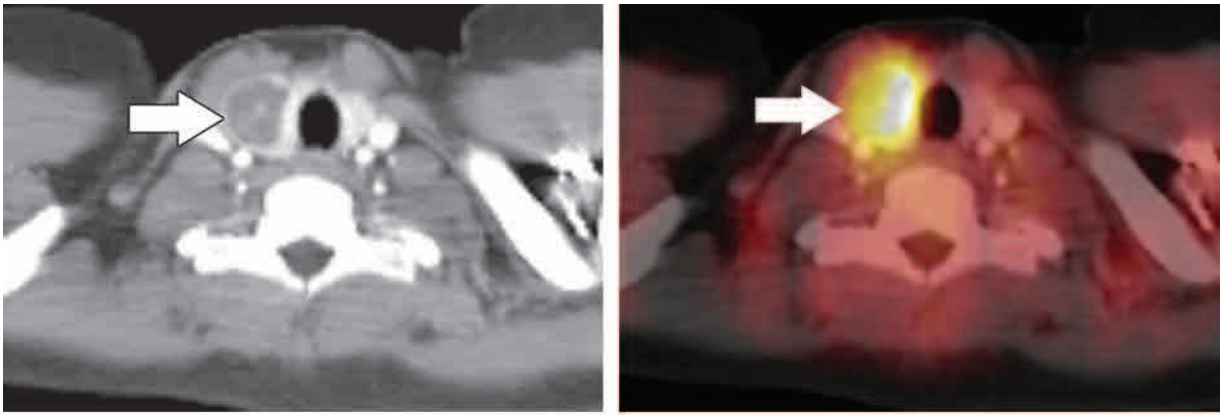

Figure 2. Hürthle cell carcinoma. Axial CT **(a)** and fused PET-CT **(b)** scans help localize a focal abnormality (arrow) to a 2.5-cm cystic thyroid mass. Biopsy of the mass helped confirm a Hürthle cell carcinoma of the thyroid gland.

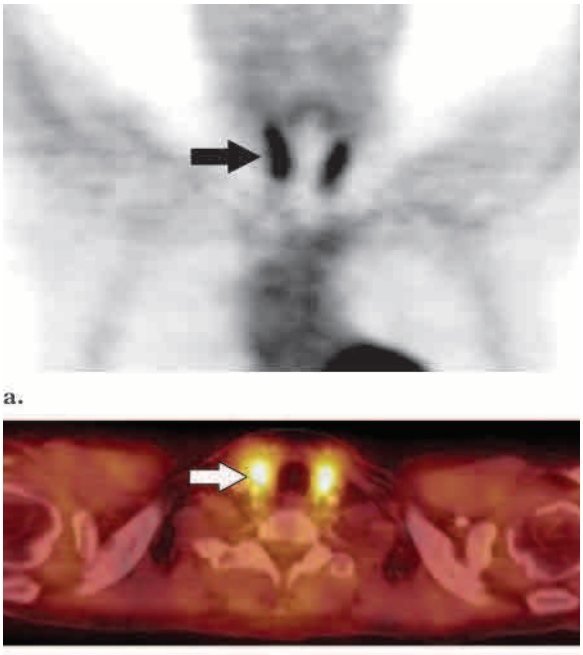

Figure 3. Physiologic thyroid uptake. **(a)** Coronal PET scan shows diffuse symmetric FDG uptake localized to the thyroid gland (arrow). **(b)** Axial fused PET-CT scan helps confirm localization of the uptake to the thyroid gland (arrow).

muscles of the oropharynx and nasopharynx, laryngeal muscles), fat, lymphoid tissue, and mucosa. We also discuss a variety of artifacts that are specific to PET-CT that may mimic either physiologic or pathologic FDG uptake.

We compiled an atlas of FDG uptake in the head and neck region on the basis of PET-CT findings in 11,000 patients. PET and CT were performed on a prototype or on a Biograph (CTI PET Systems, Knoxville, Tenn) or Reveal (Siemens Medical Systems, Florsheim, Germany) PET-CT scanner. Patients received 6–11 mCi (222–407 MBq) of FDG intravenously and were scanned after a 60-minute uptake period. Standard CT clinical protocols were used, including oral and intravenous administration of contrast material, as was CT-based attenuation correction. In general, patterns of FDG uptake were variable and often reflected patient activity (eg, talking, coughing) during or directly preceding the FDG uptake phase. Part 2 of this two-part series of articles discusses the use of combined PET-CT in patients with head and neck malignancies.

Patterns of FDG Uptake

Glands

Thyroid Gland.—The thyroid gland has a variable appearance on FDG PET scans. It can demonstrate diffuse, focal, asymmetric, or virtually no FDG uptake, and these uptake patterns can be seen in physiologic, benign, and pathologic processes (7,12–14). Focal thyroid uptake is relatively nonspecific and has been reported in benign entities such as toxic thyroid adenoma (Fig 1) as well as in thyroid malignancies (Fig 2) (15). Recently, it has been reported that focal thyroid uptake, regardless of the primary indication for the examination, may represent a second primary malignancy (16,17).

Diffuse symmetric FDG accumulation within the thyroid gland can be seen in normal glands and is occasionally seen in patients with diffuse goiters (Fig 3).

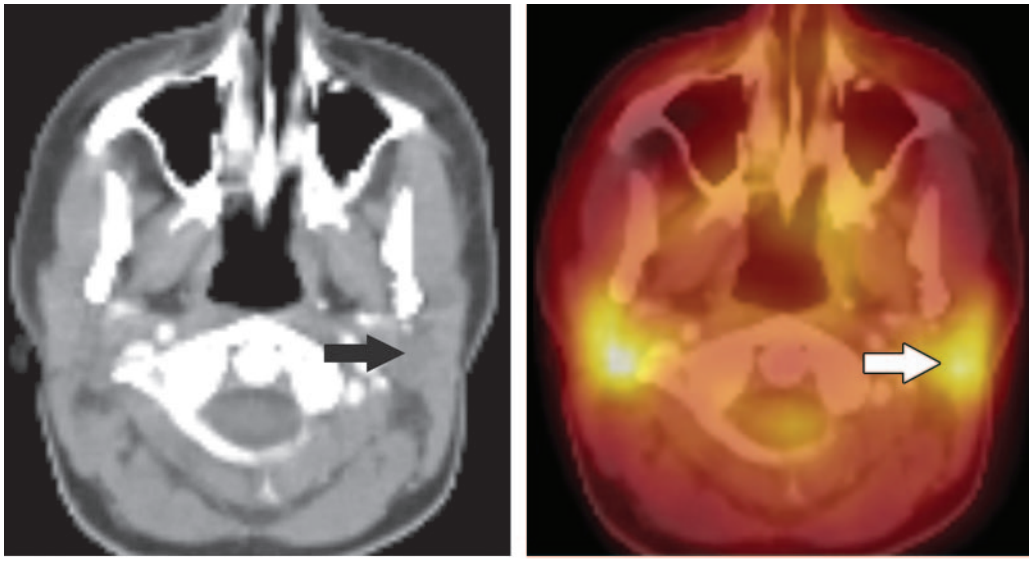

a. b.

Figure 4. Physiologic parotid uptake. Axial CT **(a)** and fused PET-CT **(b)** scans show moderate symmetric FDG uptake in the parotid glands (arrow).

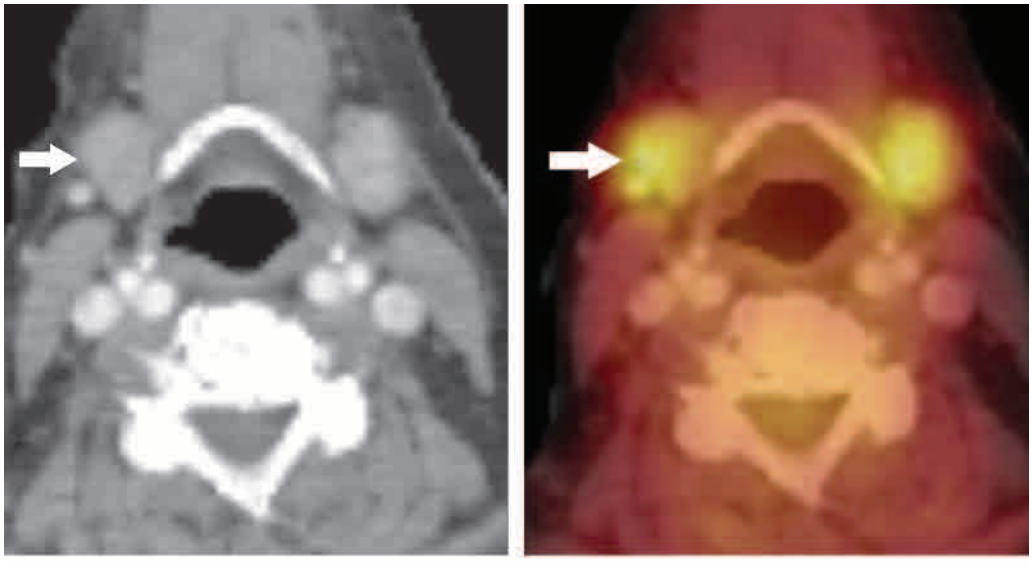

a. b.

Figure 5. Physiologic submandibular uptake. Axial CT **(a)** and fused PET-CT **(b)** scans demonstrate symmetric FDG uptake that is localized to the submandibular glands (arrow).

Although the thyroid gland can demonstrate several different patterns of FDG uptake, diffuse uptake in the thyroid gland is seen as a normal variant within normal glands, as well as in benign causes such as chronic autoimmune thyroiditis or goiter. The more problematic focal FDG uptake can be seen as a result of malignancy or adenomatous processes (17). However, because focal asymmetric uptake can represent a primary thyroid neoplasm, we recommend that all patients with thyroid nodules greater than 10 mm or with intense asymmetric FDG uptake be referred for biopsy.

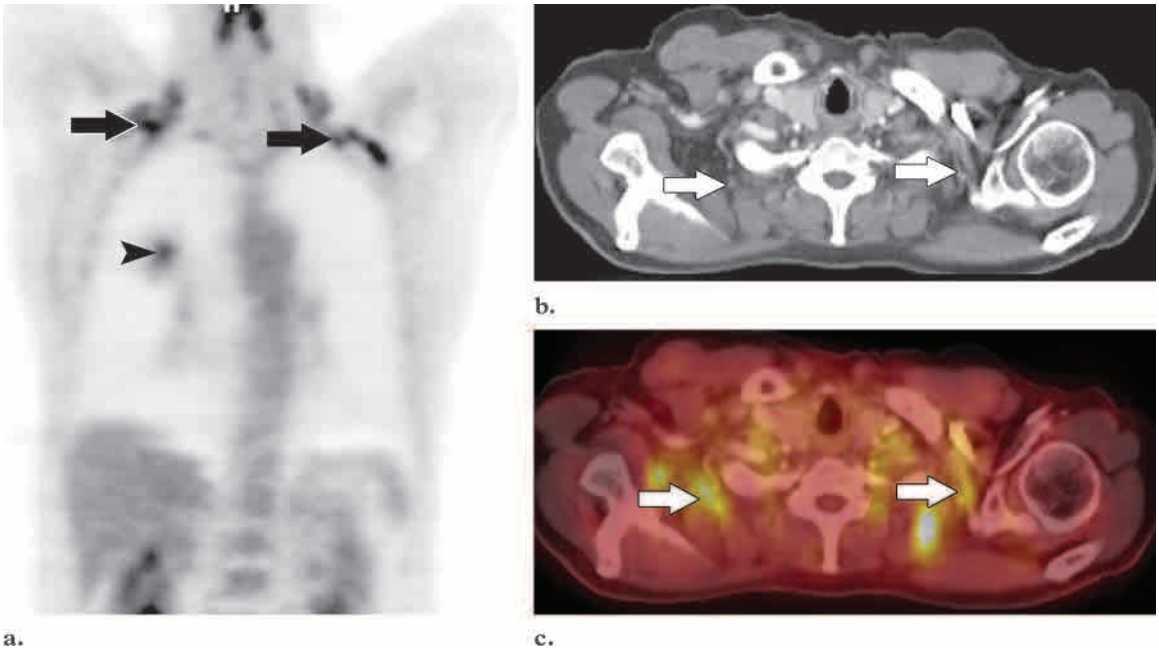

Figure 6. Physiologic muscle uptake. **(a)** Coronal PET scan demonstrates multiple bilateral foci of intense FDG uptake (arrows). Note also the primary right lung cancer (arrowhead). **(b)** Axial CT scan of the lower neck shows foci of intense FDG uptake in the shoulder girdle (arrows). **(c)** Fused PET-CT scan helps localize the foci of FDG uptake to muscles and fat in the shoulder girdle (arrows).

Salivary Glands.—FDG is taken up by the salivary glands and excreted into the saliva (18). The parotid and submandibular glands normally demonstrate mild to moderate symmetric physiologic uptake (Figs 4, 5). However, in some cases they may demonstrate little or no uptake. Asymmetric uptake can be seen in patients who have undergone surgical removal of one of the glands or in patients with primary or metastatic lesions to the glands. FDG-avid parotid tumors include Warthin tumor, pleomorphic adenoma, and primary parotid lymphoma (19–22). Nonmalignant causes of FDG uptake include infectious causes and granulomatous disorders such as sarcoidosis (23).

Benign and malignant parotid tumors cannot be distinguished with PET-CT alone because of high false-positive rates (21,24). In addition, there are several salivary gland malignancies that have little or no FDG avidity. Therefore, lack of FDG uptake within a salivary gland mass does not exclude malignancy.

Malignancy can occasionally cause bilateral FDG uptake in the parotid or submandibular glands or in intraparotid lymph nodes, mimicking a physiologic pattern of uptake. In summary, both unilateral and bilateral FDG uptake within the salivary glands can be caused by benign or malignant processes, and it is necessary to consider all available clinical information, including prior oncologic and surgical history, to make an accurate diagnosis.

Muscles

Neck and Face.—Physiologic FDG uptake within neck muscles can constitute a diagnostic dilemma in the interpretation of PET scans (7,25). Frequently, muscle uptake can be distinguished from malignant nodal uptake by identifying the characteristic pattern of linear symmetric uptake. However, muscles often demonstrate more focal uptake patterns, and combined PET-CT most frequently depicts FDG uptake localized to the myotendinous junction. These focal areas of FDG uptake can be difficult to distinguish from abnormal lymph nodes. Several foci of asymmetric uptake can be very difficult to confidently distinguish from tumor on PET scans alone (Fig 6). On PET-CT scans, these foci are easily localized to the strap muscles (particularly their insertion sites). Intense asymmetric FDG

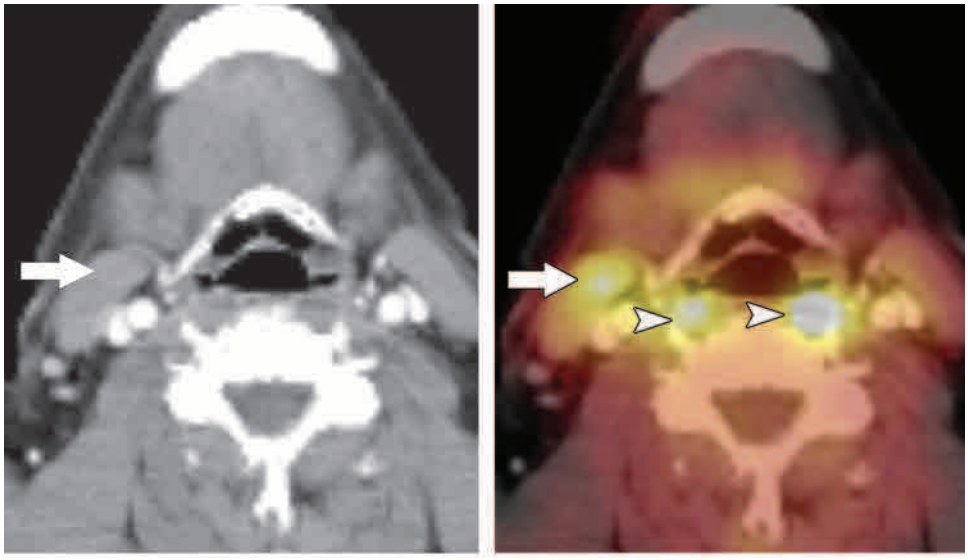

Figure 7. Asymmetric sternocleidomastoid muscle uptake. Coronal PET demonstrated asymmetric FDG uptake in the right side of the neck. **(a)** Axial CT scan shows focal FDG uptake in the right sternocleidomastoid muscle (arrow). **(b)** Corresponding fused PET-CT scan helps accurately localize the FDG uptake to the right sternocleidomastoid muscle (arrow). Note also the symmetric FDG uptake within the prevertebral muscles (arrowheads).

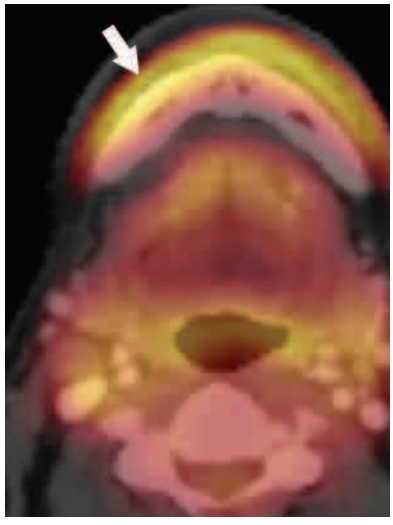

Figure 9. Physiologic facial muscle uptake. Axial fused PET-CT scan helps localize linear FDG uptake to the muscles of facial expression in the lower part of the face (arrow), a finding that is consistent with physiologic FDG uptake.

uptake can also be seen within the sternocleidomastoid muscle (Fig 7) and can mimic an enlarged lymph node. Often, inspection of coronal or sagittal reconstructed images will facilitate characterization of muscle uptake by revealing the linearity on one or more images.

Another muscle frequently demonstrating asymmetric radiotracer uptake is the inferior obliquus capitus muscle (Fig 8). Uptake within this muscle may appear focal on coronal images, but its linear nature is evident when the uptake is viewed in an axial plane. The extreme posterior position of these paraspinal muscles is also often helpful in identifying the source of the FDG uptake. The muscles of facial expression may also demonstrate linear FDG uptake (Fig 9).

Because most muscles in the neck can display asymmetric FDG uptake, both physiologically and after strain, close inspection of images obtained in all three orthogonal planes is essential to avoid misdiagnosis. Although several methods have been used to minimize muscle uptake, including the use of soft collars and benzodiazepines during the uptake phase, these techniques are inconvenient to the patient and are often not completely effective (8).

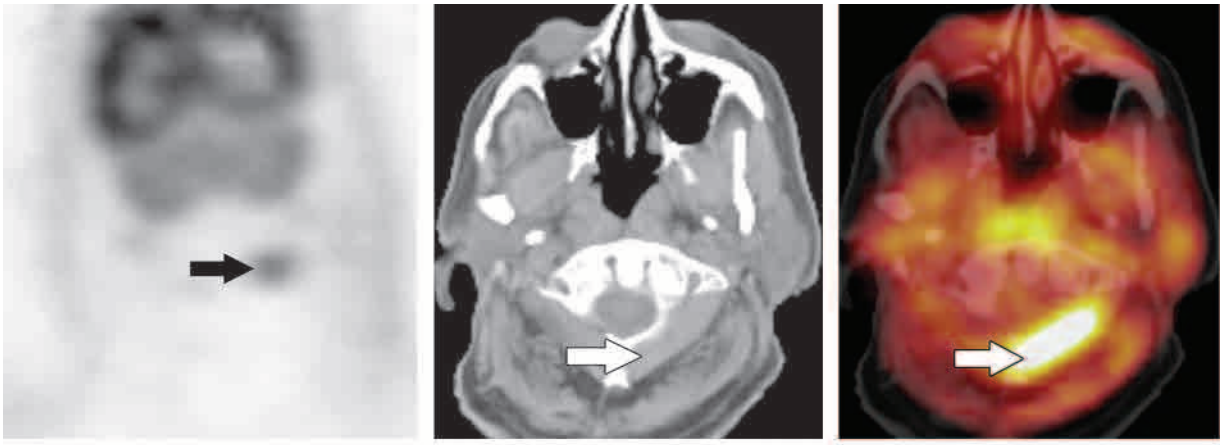

Figure 8. Asymmetric uptake in the inferior obliquus capitus muscle. **(a)** Coronal PET scan shows a hypermetabolic focus in the left side of the neck (arrow). **(b)** Axial CT scan reveals no correlative abnormality. Arrow indicates the left inferior obliquus capitus muscle. **(c)** Axial fused PET-CT scan helps confirm prominent asymmetric physiologic FDG uptake in the left inferior obliquus capitus muscle (arrow).

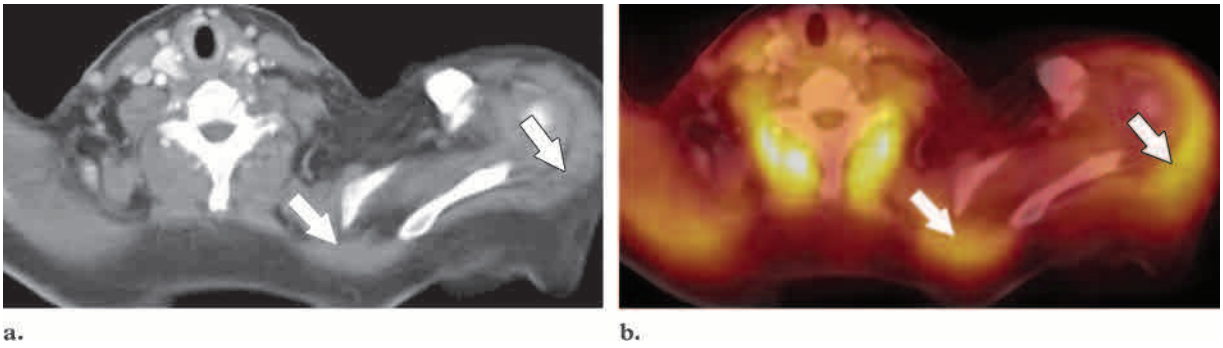

Figure 10. Physiologic effect of insulin on FDG muscle uptake. Axial CT **(a)** and fused PET-CT **(b)** scans show prominent linear FDG uptake within the muscles of the neck and upper back (arrows). The patient had received insulin prior to the injection of FDG.

Insulin mediates the entry of glucose as well as FDG into both muscle and adipose tissue. In hyperglycemic patients, insulin can be administered before FDG administration help decrease blood glucose levels. Unfortunately, insulin administration drives both glucose and FDG into the muscles, which may interfere with the evaluation of surrounding structures. Although some authors advocate administering a small dose of insulin to reduce the blood sugar level in hyperglycemic patients, in our opinion, this will not improve image quality and will, in fact, often cause image degradation from increased FDG accumulation in muscle and fat (Fig 10). At our institution, patients with mildly elevated glucose levels (<200 mg/dL) are scanned without intervention, and patients with markedly elevated glucose levels (>200–250 mg/dL) are rescheduled for later scanning if reasonably convenient for the patient.

Oropharynx and Nasopharynx.—Several muscles of the oropharynx and hypopharynx demonstrate symmetric physiologic FDG uptake, including the pterygoid muscles (Fig 11) and the muscles of the oral floor (Fig 12). When asymmetric, uptake in these locations may mimic focal areas of malignancy (Figs 13, 14).

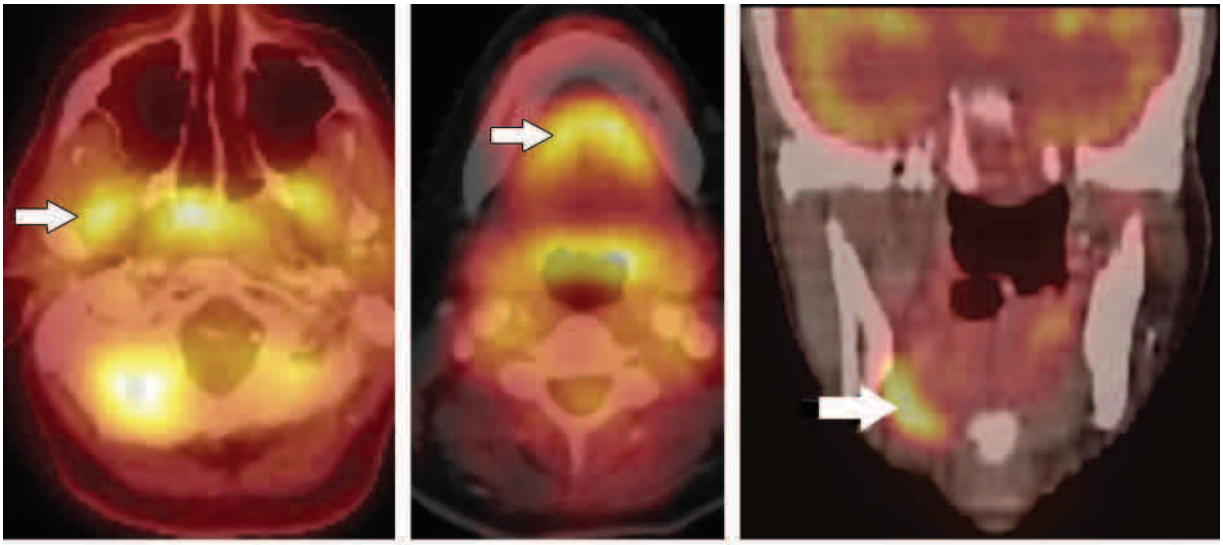

11. 12. 13.

Figures 11–13. **(11)** Physiologic lateral pterygoid muscle uptake. Coronal PET demonstrated bilateral foci of intense physiologic FDG uptake in the infratemporal fossa and adenoids. CT findings were normal. Axial fused PET-CT scan helps localize foci of uptake to the superior portion of the lateral pterygoid muscles (arrow). **(12)** Symmetric physiologic mylohyoid muscle uptake. Axial fused PET-CT scan helps accurately localize FDG uptake to the mylohyoid line (the insertion site of the mylohyoid muscle) (arrow). **(13)** Asymmetric mylohyoid muscle uptake. Coronal fused PET-CT scan demonstrates precise localization of FDG to the right mylohyoid muscle (arrow).

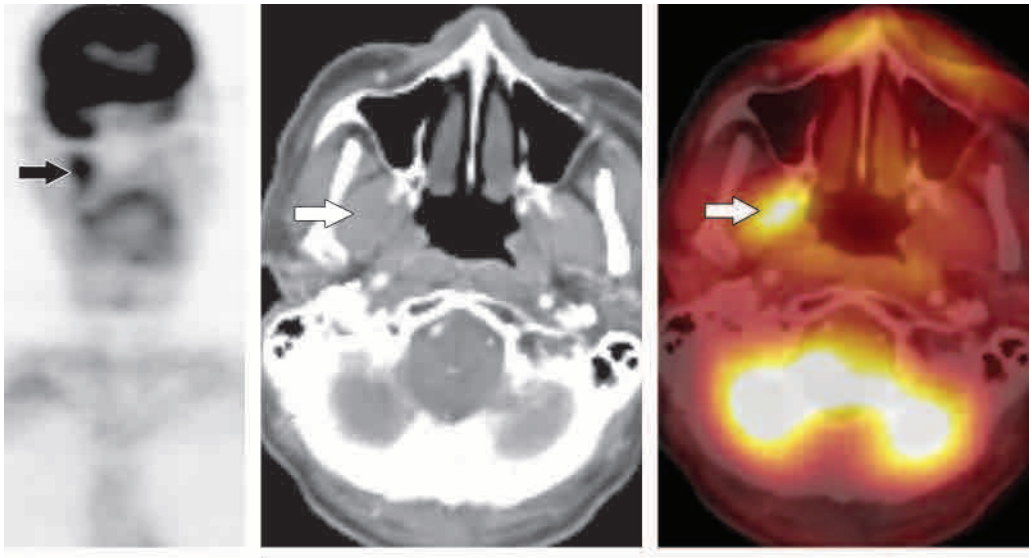

a. b. c.

Figure 14. Asymmetric uptake in the right medial pterygoid muscle. **(a)** Coronal PET scan shows a large, asymmetric hypermetabolic focus in the right infratemporal fossa (arrow). **(b)** Axial CT scan demonstrates no abnormality. Arrow indicates the right medial pterygoid muscle. **(c)** Axial fused PET-CT scan helps accurately localize uptake to the right medial pterygoid muscle (arrow), a finding that is consistent with asymmetric physiologic muscle uptake.

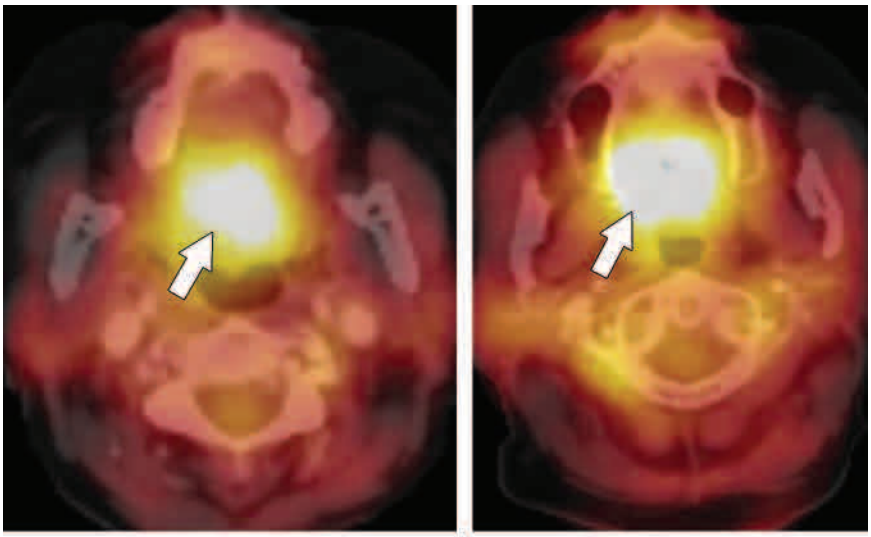

15. 16.

Figures 15, 16. **(15)** Lingual uptake. Axial fused PET-CT scan demonstrates physiologic lingual FDG uptake (arrow). **(16)** Palatal mucosal uptake. Axial fused PET-CT scan shows intense FDG uptake in the superior oropharynx (arrow). FDG uptake within the mucosa of the soft palate is often indistinguishable from the slightly more inferior lingual uptake (cf Fig 15).

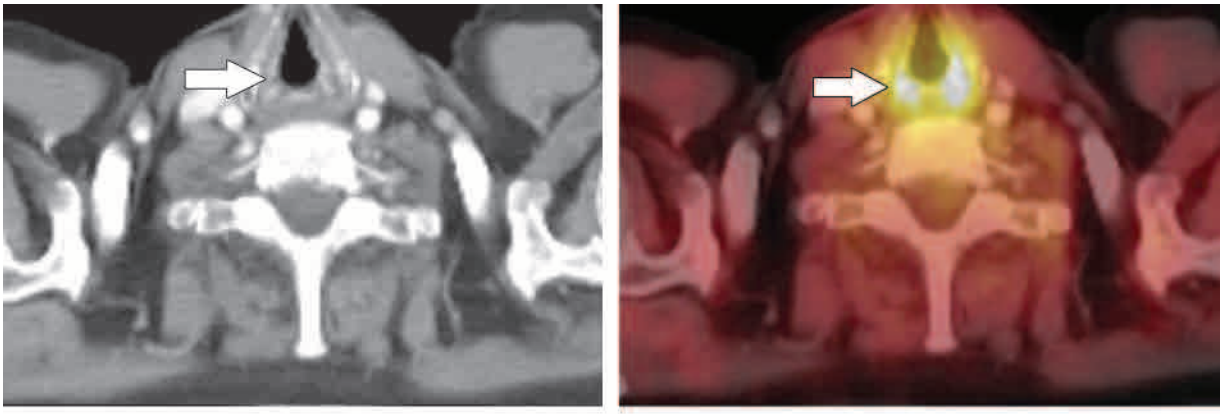

a. b.

Figure 17. Physiologic vocal cord uptake. Axial CT **(a)** and fused PET-CT **(b)** scans help identify FDG uptake in the neck as symmetric physiologic activity in the true vocal cords (arrow). The patient was talking during the uptake phase.

Lingual FDG uptake is also common and may appear diffuse or as focal bilaterally symmetric uptake. Lingual uptake is often indistinguishable from the slightly more superior palatal mucosal uptake on PET scans alone but can typically be differentiated on fused PET-CT scans (Figs 15, 16).

Larynx.—It is well recognized that talking during the FDG uptake phase will cause radiotracer accumulation in the muscles of phonation and the vocal cords (Fig 17). Another muscle that can

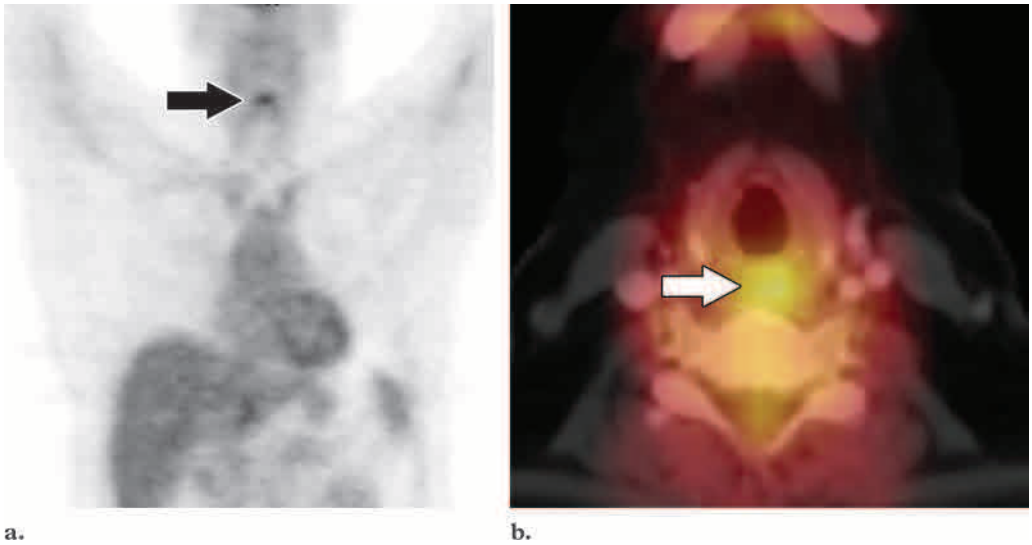

Figure 18. Physiologic cricopharyngeus muscle uptake. **(a)** Coronal PET scan demonstrates a hypermetabolic focus (arrow). **(b)** Axial fused PET-CT scan helps localize the area of uptake precisely to the cricopharyngeus muscle (arrow).

appear as a focal area of FDG uptake is the cricopharyngeus muscle (Fig 18) (26). Coughing during the uptake phase produces FDG activity in the pharyngeal constrictor muscles as well as in the vocal cords (Fig 19). Pronounced uptake in these muscles can interfere with interpretation of PET scans in any patient, but especially in patients with head and neck malignancies, thyroid cancer, or lymphoma, in whom it can be very difficult to distinguish physiologic muscle uptake from pathologic uptake (27,28).

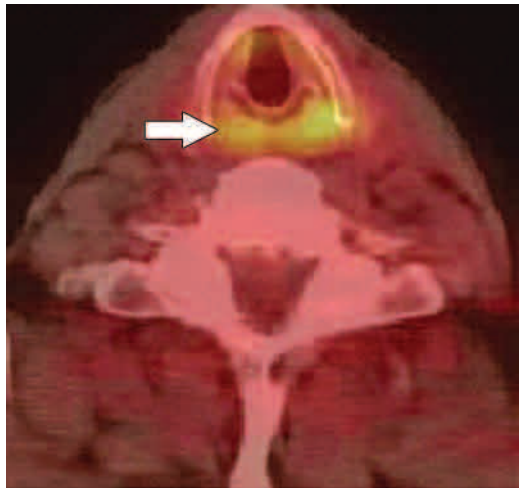

Figure 19. Pharyngeal constrictor muscle uptake. Axial fused PET-CT scan demonstrates physiologic FDG uptake within the pharyngeal constrictor muscles (arrow). The patient was coughing during the uptake phase.

Fat

Until recent reports of FDG uptake by brown fat, most of the linear and focal uptake in the neck that had the characteristic appearance of muscle was attributed to muscle alone. After the implementation of combined PET-CT, it became apparent that uptake previously attributed to muscle had no definite soft tissue–muscle correlation when the fused PET-CT scans were inspected. Several authors have recently reported intense FDG uptake within fat, presumably brown fat (Fig 20) (29–31). The question of whether the FDG uptake is in fat or muscle has little clinical relevance; however, the foregoing discussion illustrates how mislocalization of physiologic FDG accumulation can be rectified with combined PET-CT. The way to determine whether an area of FDG uptake correlates with fat is to measure the attenuation, which should be between −50 and −150 HU (ie, fat attenuation).

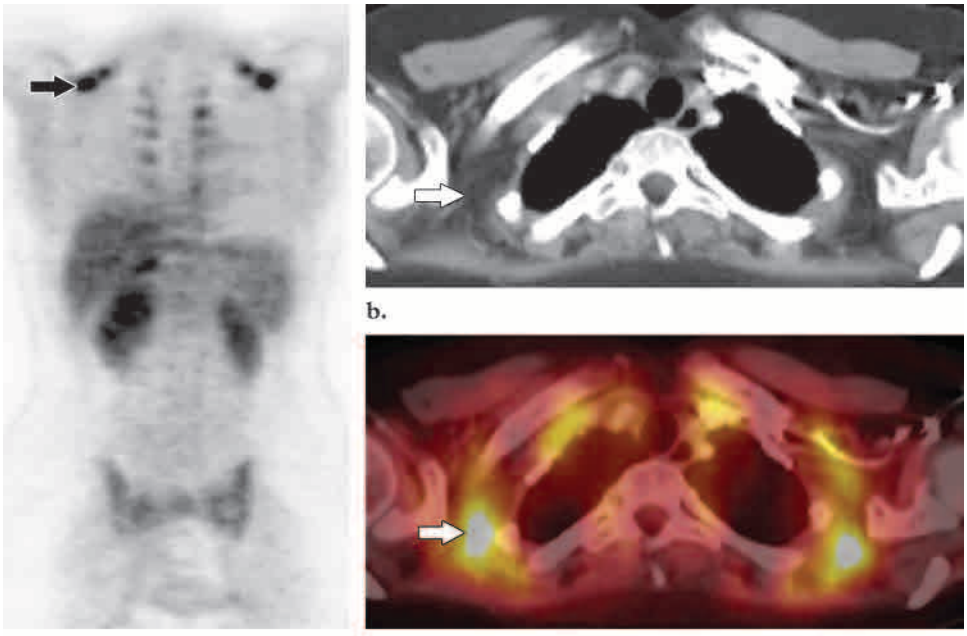

Figure 20. Physiologic brown fat uptake. **(a)** Coronal PET scan shows bilateral foci of intense FDG uptake in the posterior superior thorax (arrow). **(b)** Axial CT scan shows no correlative abnormality. Arrow indicates an area of fat attenuation. **(c)** Axial fused PET-CT scan helps localize the foci precisely to areas of fat attenuation seen at CT (arrow).

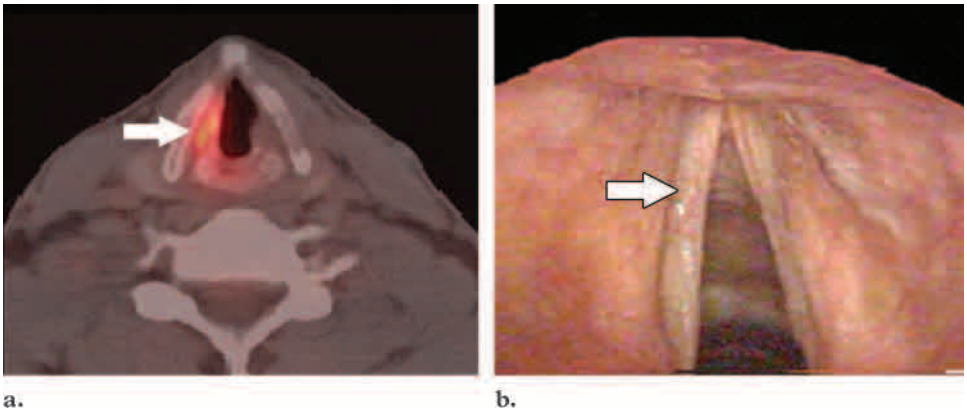

Figure 21. Asymmetric superphysiologic uptake in a vocal cord following paralysis of the contralateral cord caused during thyroid surgery. **(a)** Axial fused PET-CT scan helps localize asymmetric FDG uptake to the right true vocal cord (arrow), a finding that simulates a laryngeal neoplasm. **(b)** Laryngoscopic image helps confirm superphysiologic metabolic activity in the normal vocal cord (arrow) and paralysis of the contralateral cord. (Figure 21 reprinted, with permission, from reference 33.)

Postoperative Alterations

Knowledge of prior surgeries and of surgical complications is essential for properly interpreting FDG uptake in the head and neck. Several cases of asymmetric vocal cord uptake following injury to the recurrent laryngeal nerve have been reported (32,33). This phenomenon is the result of altered physiologic or superphysiologic uptake due to compensation of the contralateral vocal cord during phonation (33). Asymmetric FDG uptake within a single vocal cord can mimic malignancy, especially at PET, if direct anatomic correlation is not available. Localizing asymmetric FDG uptake within a vocal cord is much less of a diagnostic problem when using PET-CT (Fig 21).

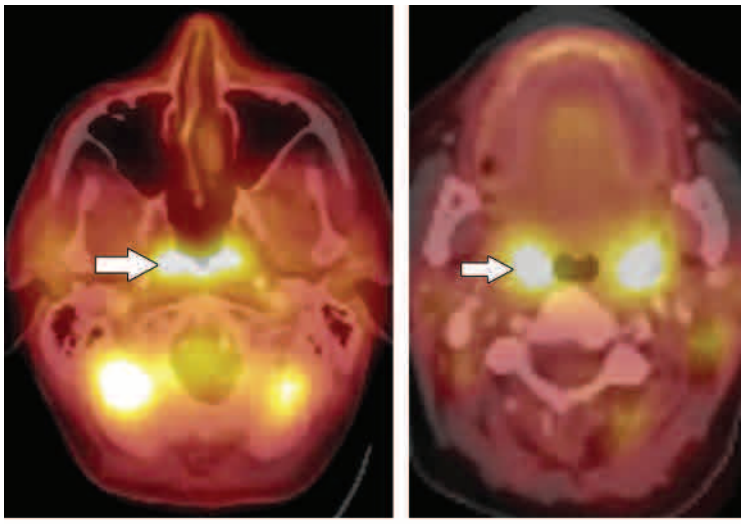

22. 23.

Figures 22, 23. **(22)** Physiologic adenoid uptake. Axial fused PET-CT scan helps localize intense bilateral nasopharyngeal FDG uptake to the adenoids (arrow). **(23)** Physiologic palatine tonsil uptake. Axial fused PET-CT scan shows intense symmetric physiologic FDG uptake within the palatine tonsils (arrow). This finding can also be seen in tonsillar hyperplasia.

Figure 24. Squamous cell carcinoma of the nasopharynx in a patient with squamous cell metastases to the neck and no known primary malignancy. Axial fused PET-CT scan shows asymmetric FDG uptake in the left side of the nasopharynx (arrow). Subsequent biopsy helped confirm the diagnosis.

Lymphoid Tissue

There are many lymphatic structures in the head and neck, including the Waldeyer ring (adenoids, palatine tonsils, lingual tonsils), lymph nodes, and lymphatic channels (Figs 22, 23). Physiologic FDG uptake can be seen in any lymphatic structure in the head and neck, due at least in part to accumulation of FDG within macrophages and lymphocytes. Several authors have described physiologic FDG uptake within these structures on dedicated PET scans (4,7,34,35). The interpretation is straightforward in most cases, especially when there is symmetric uptake. However, malignancy or hyperplasia may have a similar symmetric appearance.

Uptake in the Waldeyer ring will often be asymmetric, even from benign conditions such as infection or inflammation. Malignancy will usually manifest as asymmetric FDG uptake as well, with or without significant anatomic abnormalities (Fig 24).

When it infiltrates into the subcutaneous tissues, FDG can be transported through the lymphatic system, causing a lymphangiographic effect at PET. If FDG infiltrates into the soft tissues of the upper extremity, it may accumulate in axillary or supraclavicular lymph nodes, which may necessitate repeat scanning (Fig 25).

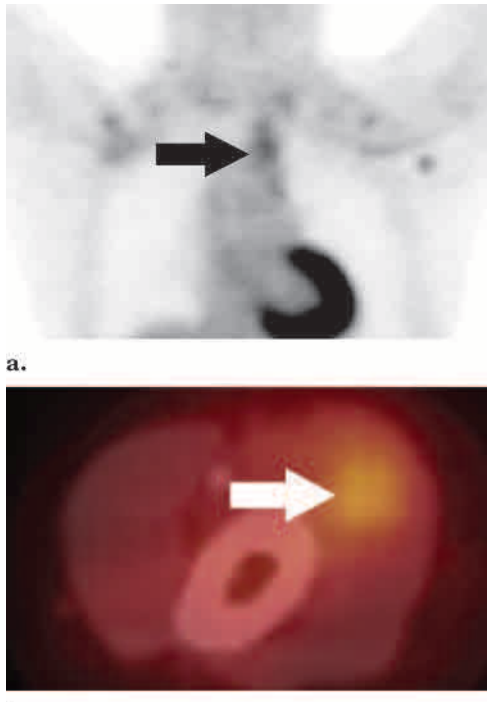

a. b.

Figure 25. Lymphangiographic effect in a patient with known infiltration of FDG into the left antecubital vein. **(a)** Coronal PET scan shows accumulation of FDG within the axillary and left paratracheal lymph nodes (arrow). **(b)** Axial fused PET-CT scan of the left arm shows indistinct areas of FDG accumulation within the lymphatic channels (arrow). Repeat fused PET-CT performed a few weeks later showed no evidence of nodal uptake.

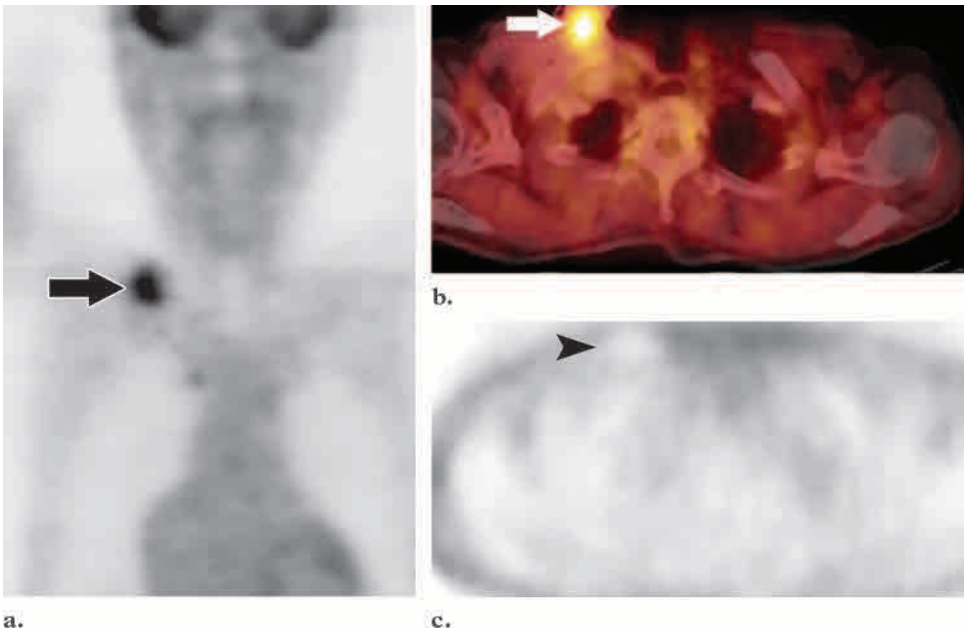

Figure 26. CT attenuation artifact from an implantable catheter port. **(a)** Coronal PET scan demonstrates focal intense FDG accumulation in the right supraclavicular area (arrow). **(b)** Axial fused PET-CT scan helps localize the FDG activity to an implanted catheter port (arrow). **(c)** Axial uncorrected emission image helps confirm that the abnormality (arrowhead) is an attenuation correction artifact caused by the extremely high attenuation of the port.

Mucosa

The mucosa of the oropharynx and nasopharynx often demonstrates physiologic FDG uptake. This uptake does not usually cause problems with interpretation because it is almost invariably located superficially along the mucosal plane and linear in configuration (Fig 16).

PET-CT Artifacts

Several artifacts inherent in PET have been described, including prominent skin activity on nonattenuation-corrected images and relatively photopenic areas due to prosthetic devices (12,36). These artifacts are present on fused PET-CT scans as well. However, there are a number of "new" artifacts that are unique to combined PET-CT. These artifacts are not generated on PET scanners, which use point source–based systems for attenuation correction, because they are generated by CT-based attenuation correction protocols.

Metallic devices, including dental implants, create areas of photopenia on PET scans. These areas remain photopenic on attenuation-corrected images when Germanium point sources are used for attenuation correction. In contrast, with use of current CT-based attenuation correction algorithms, these areas can demonstrate falsely elevated FDG uptake (Fig 26). This artifact is a limitation of the current CT attenuation correction protocols.

Intravenous contrast material can also cause artifacts on attenuation-corrected images when CT-based attenuation correction protocols are used. Dense contrast material is present in venous structures during CT but not during the PET portion of the examination. This mismatch causes areas of linear artifact (mimicking intense FDG accumulation) on the attenuation-corrected PET

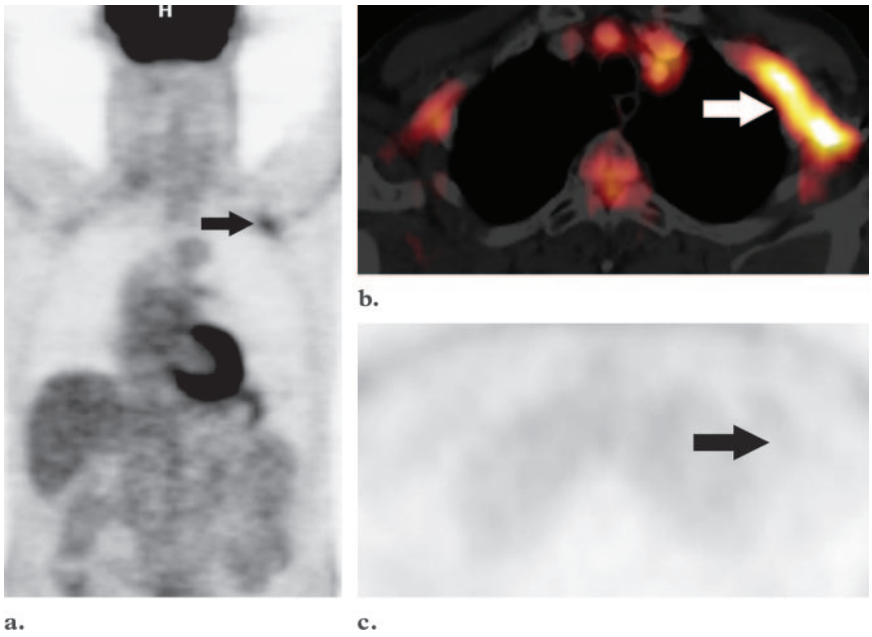

Figure 27. Linear CT attenuation artifact due to high-attenuation intravenous contrast material. **(a)** Coronal PET scan shows a focal area of intense FDG accumulation located in the left axilla (arrow) and mimicking an abnormal axillary lymph node. **(b)** Axial fused PET-CT scan helps localize the uptake to an area of dense contrast material in the left subclavian vein (arrow). **(c)** Axial uncorrected emission image reveals that the area of apparent FDG uptake in the axilla (arrow) is an artifact generated during the attenuation correction process. (Figure 27 reprinted, with permission, from reference 37.)

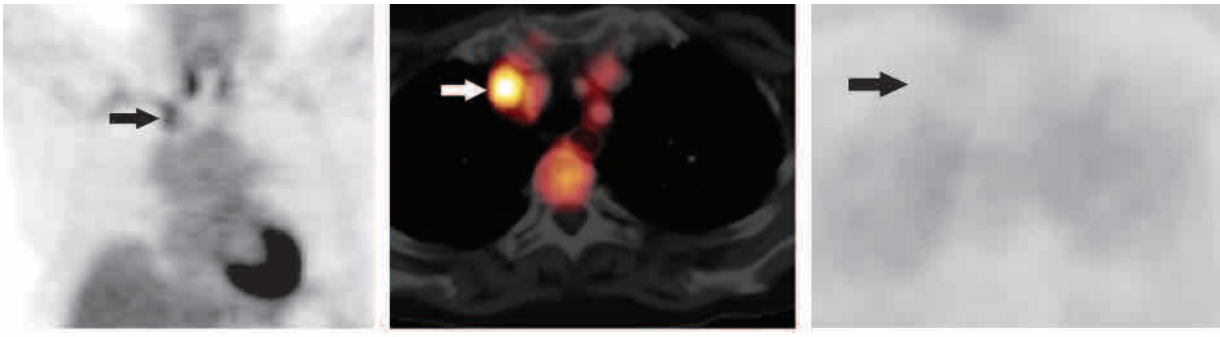

Figure 28. Focal CT attenuation artifact due to high-attenuation intravenous contrast material. **(a)** Coronal PET scan shows symmetric FDG uptake in the thyroid gland and a focal area of intense uptake in the right supraclavicular region (arrow) mimicking an abnormal lymph node. **(b)** Axial fused PET-CT scan helps localize the apparent FDG activity precisely to the brachiocephalic vein (arrow). **(c)** On an axial uncorrected emission image, no apparent FDG activity is seen (arrow), indicating that the area of uptake seen at fused PET-CT represents an artifact of CT-based attenuation correction.

scans (Fig 27). Occasionally, this artifact can appear focal and mimic a metastatic lymph node in the axilla or supraclavicular area (Fig 28) (10). Rarely, a small malignant lymph node or small soft-tissue abnormality can lie within or directly beside a contrast material–related artifact, which then partially or completely obscures the abnormality (Fig 29). A relatively simple means of resolving any diagnostic uncertainty regarding the presence of a CT-based attenuation artifact is inspection of the emission data set (ie, non-attenuation-corrected PET scan). Unfortunately,

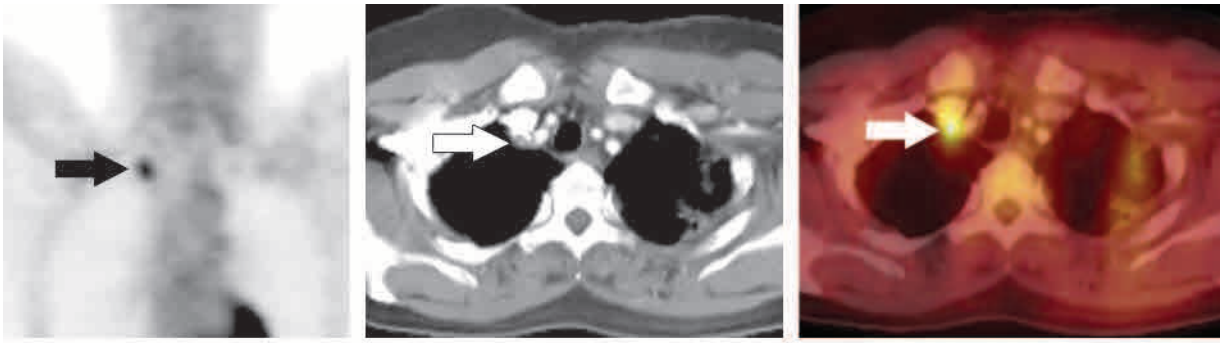

Figure 29. Abnormal lymph node adjacent to high-attenuation intravenous contrast material. **(a)** Coronal PET scan shows a small focal abnormality in the supraclavicular region (arrow). **(b, c)** Axial CT **(b)** and fused PET-CT **(c)** scans help localize the abnormality to the right brachiocephalic vein (cf Fig 28). In this case, however, uncorrected emission PET still showed the abnormality, indicating that the abnormality did not represent an attenuation correction artifact, but rather a small node adjacent to the brachiocephalic vein.

with some viewing systems it can be cumbersome to switch between the attenuation-corrected PET image sets and the emission-only data sets. In addition, some systems will not allow side-by-side comparison of corrected and uncorrected images.

Although one group has reported that the use of oral contrast material does not cause attenuation artifacts, another has reported that areas of highly concentrated barium-based oral contrast material within the bowel can cause similar artifacts and overestimation of FDG activity in the bowel by as much as 20% (38,39). The same group has proposed a complex region-growing and segmentation CT-based attenuation correction algorithm that appears to correct most, if not all, of the CT-based attenuation artifacts.

Conclusions

Combined PET-CT is a unique imaging modality that permits anatomic (CT) and functional (PET) scans to be acquired with perfect or near-perfect coregistration using a single device. Combined PET-CT offers additional information that cannot be obtained with PET or CT alone. In particular, PET-CT facilitates the interpretation of FDG uptake in the head and neck, an area of particular difficulty due to dense and complex anatomic structures.

We have presented an index of FDG uptake in the head and neck, covering physiologic FDG uptake and uptake due to altered physiologic states, and have discussed artifacts in the head and neck that are unique to PET-CT scanners. With the burgeoning interest in these scanners, it is imperative that interpreting radiologists and nuclear medicine physicians be familiar with the patterns of FDG uptake in the head and neck to avoid misinterpretation or misdiagnosis.

References

1. Dizendorf EV, Baumert BG, Von Schulthess GK, Lutolf UM, Steinert HC. Impact of whole-body (18)F-FDG PET on staging and managing patients for radiation therapy. J Nucl Med 2003; 44: 24–29.
2. Hannah A, Scott AM, Tochon-Danguy H, et al. Evaluation of 18 F-fluorodeoxyglucose positron emission tomography and computed tomography with histopathologic correlation in the initial staging of head and neck cancer. Ann Surg 2002; 236: 208–217.
3. Lowe VJ, Boyd JH, Dunphy FR, et al. Surveillance for recurrent head and neck cancer using positron emission tomography. J Clin Oncol 2000; 18:651–658.
4. Hanasono MM, Kunda LD, Segall GM, Ku GH, Terris DJ. Uses and limitations of FDG positron emission tomography in patients with head and neck cancer. Laryngoscope 1999; 109:880–885.
5. Farber LA, Benard F, Machtay M, et al. Detection of recurrent head and neck squamous cell carcinomas after radiation therapy with 2–18F-fluoro-2-deoxy-D-glucose positron emission tomography. Laryngoscope 1999; 109:970–975.
6. Jabour BA, Choi Y, Hoh CK, et al. Extracranial head and neck: PET imaging with 2-[F-18]fluoro-2-deoxy-D-glucose and MR imaging correlation. Radiology 1993; 186:27–35.
7. Shreve PD, Anzai Y, Wahl RL. Pitfalls in oncologic diagnosis with FDG PET imaging: physiologic and benign variants. RadioGraphics 1999; 19:61–77.
8. Barrington SF, Maisey MN. Skeletal muscle uptake of fluorine-18-FDG: effect of oral diazepam. J Nucl Med 1996; 37:1127–1129.
9. Kinahan PE, Townsend DW, Beyer T, Sashin D. Attenuation correction for a combined 3D PET/CT scanner. Med Phys 1998; 25:2046–2053.
10. Antoch G, Freudenberg LS, Egelhof T, et al. Focal tracer uptake: a potential artifact in contrast-enhanced dual-modality PET/CT scans. J Nucl Med 2002; 43:1339–1342.

11. Goerres GW, Hany TF, Kamel E, von Schulthess GK, Buck A. Head and neck imaging with PET and PET/CT: artefacts from dental metallic implants. Eur J Nucl Med Mol Imaging 2002; 29: 367–370.
12. Cook GJ, Fogelman I, Maisey MN. Normal physiological and benign pathological variants of 18-fluoro-2-deoxyglucose positron-emission tomography scanning: potential for error in interpretation. Semin Nucl Med 1996; 26:308–314.
13. Gordon BA, Flanagan FL, Dehdashti F. Whole-body positron emission tomography: normal variations, pitfalls, and technical considerations. AJR Am J Roentgenol 1997; 169:1675–1680.
14. Lin EC. Thyroid nodule mimicking cervical adenopathy on FDG positron emission tomographic imaging. Clin Nucl Med 2002; 27:656–657.
15. Borner AR, Voth E, Wienhard K, Wagner R, Schicha H. F-18-FDG PET in autonomous goiter. Nuklearmedizin 1999; 38:1–6.
16. Ramos CD, Chisin R, Yeung HW, Larson SM, Macapinlac HA. Incidental focal thyroid uptake on FDG positron emission tomographic scans may represent a second primary tumor. Clin Nucl Med 2001; 26:193–197.
17. McDougall IR, Davidson J, Segall GM. Positron emission tomography of the thyroid, with an emphasis on thyroid cancer. Nucl Med Commun 2001; 22:485–492.
18. Stahl A, Dzewas B, Schwaiger M, Weber WA. Excretion of FDG into saliva and its significance for PET imaging. Nuklearmedizin 2002; 41:214–216.
19. Horiuchi M, Yasuda S, Shohtsu A, Ide M. Four cases of Warthin's tumor of the parotid gland detected with FDG PET. Ann Nucl Med 1998; 12: 47–50.
20. Matsuda M, Sakamoto H, Okamura T, et al. Positron emission tomographic imaging of pleomorphic adenoma in the parotid gland. Acta Otolaryngol Suppl 1998; 538:214–220.
21. Okamura T, Kawabe J, Koyama K, et al. Fluorine-18 fluorodeoxyglucose positron emission tomography imaging of parotid mass lesions. Acta Otolaryngol Suppl 1998; 538:209–213.
22. Shih WJ, Ghesani N, Hongming Z, Alavi A, Schusper S, Mozley D. F-18 FDG positron emission tomography demonstrates resolution of non-Hodgkin's lymphoma of the parotid gland in a patient with Sjogren's syndrome: before and after anti-CD20 antibody rituximab therapy. Clin Nucl Med 2002; 27:142–143.
23. Sagowski C, Ussmuller J. Clinical diagnosis of salivary gland sarcoidosis (Heerfordt syndrome). HNO 2000; 48:613–615.
24. Keyes JW Jr, Harkness BA, Greven KM, Williams DW 3rd, Watson NE Jr, McGuirt WF. Salivary gland tumors: pretherapy evaluation with PET. Radiology 1994; 192:99–102.
25. Bar-Shalom R. Muscle uptake of 18-fluorine fluorodeoxyglucose. Semin Nucl Med 2000; 30:306–309.
26. Kostakoglu L, Wong JC, Barrington SF, Cronin BF, Dynes AM, Maisey MN. Speech-related visualization of laryngeal muscles with fluorine-18-FDG. J Nucl Med 1996; 37:1771–1773.
27. Igerc I, Kumnig G, Heinisch M, Kresnik E, Mikosch P, Gallowitsch HJ, et al. Vocal cord muscle activity as a drawback to FDG-PET in the followup of differentiated thyroid cancer. Thyroid 2002; 12:87–89.
28. Zhu Z, Chou C, Yen TC, Cui R. Elevated F-18 FDG uptake in laryngeal muscles mimicking thyroid cancer metastases. Clin Nucl Med 2001; 26: 689–691.
29. Cohade C, Osman M, Pannu HK, Wahl RL. Uptake in supraclavicular area fat ("USA-Fat"): description on 18F-FDG PET/CT. J Nucl Med 2003; 44:170–176.
30. Virtanen KA, Peltoniemi P, Marjamaki P, et al. Human adipose tissue glucose uptake determined using [(18)F]-fluoro-deoxy-glucose ([(18)F]FDG) and PET in combination with microdialysis. Diabetologia 2001; 44:2171–2179.
31. Hany TF, Gharehpapagh E, Kamel EM, Buck A, Himms-Hagen J, von Schulthess GK. Brown adipose tissue: a factor to consider in symmetrical tracer uptake in the neck and upper chest region. Eur J Nucl Med Mol Imaging 2002; 29:1393–1398.
32. Kamel EM, Goerres GW, Burger C, von Schulthess GK, Steinert HC. Recurrent laryngeal nerve palsy in patients with lung cancer: detection with PET-CT image fusion—report of six cases. Radiology 2002; 224:153–156.
33. Heller MT, Meltzer CC, Fukui MB, et al. Superphysiologic FDG uptake in the non-paralyzed vocal cord: resolution of a false-positive PET result with combined PET-CT imaging. Clin Positron Imaging 2000; 3:207–211.
34. Stokkel MP, Bongers V, Hordijk GJ, van Rijk PP. FDG positron emission tomography in head and neck cancer: pitfall or pathology? Clin Nucl Med 1999; 24:950–954.
35. Kawabe J, Okamura T, Shakudo M, et al. Physiological FDG uptake in the palatine tonsils. Ann Nucl Med 2001; 15:297–300.
36. Puthenpurayil K, Blodgett TM, Meltzer CC. Photopenic defects in FDG PET scanning. AUR Annual Meeting, 2002.
37. Fukui MB, Blodgett TM, Meltzer CC. PET/CT imaging in recurrent head and neck cancer. Semin Ultrasound CT MR 2003; 24:157–163.
38. Dizendorf EV, Treyer V, Von Schulthess GK, Hany TF. Application of oral contrast media in coregistered positron emission tomography-CT. AJR Am J Roentgenol 2002; 179:477–481.
39. Carney JP, Brasse D, Yap JT, Townsend DW. Clinical PET/CT scanning using oral CT contrast agents (abstr). J Nucl Med 2002; 45:57.

This article meets the criteria for 1.0 category 1 credit toward the AMA Physician's Recognition Award. To obtain credit, see www.rsna.org/education/rg_cme.html.